



ELSEVIER

The structural basis of substrate translocation by the *Escherichia coli* glycerol-3-phosphate transporter: a member of the major facilitator superfamily

M Joanne Lemieux^{1,2}, Yafei Huang¹ and Da-Neng Wang^{1*}

The major facilitator superfamily represents the largest group of secondary active membrane transporters in the cell. The 3.3 Å resolution structure of a member of this protein superfamily, the glycerol-3-phosphate transporter from the *Escherichia coli* inner membrane, reveals two domains connected by a long central loop. These N- and C-terminal domains, each containing a six-helix bundle, are related by pseudo-twofold symmetry. A substrate translocation pore is located between the two domains and is open to the cytoplasm. Two arginines at the closed end of the pore comprise the substrate-binding site. Biochemical experiments show that, upon substrate binding, the protein adopts a more compact conformation. The crystal structure suggests that the transporter operates through a single binding site, alternating access mechanism via a rocker-switch type of movement of the N- and C-terminal domains. The structure and mechanism of the glycerol-3-phosphate transporter form a paradigm for other members of the major facilitator superfamily.

Addresses

¹ Skirball Institute of Biomolecular Medicine and Department of Cell Biology, New York University School of Medicine, 540 First Avenue, New York, New York 10016, USA

² Current address: Department of Biochemistry, University of Alberta, Edmonton, T6G 2H7, Canada

*e-mail: wang@saturn.med.nyu.edu

Current Opinion in Structural Biology 2004, 14:405–412

This review comes from a themed issue on
Membranes
Edited by So Iwata and H Ronald Kaback

Available online 28th July 2004

0959-440X/\$ – see front matter
© 2004 Elsevier Ltd. All rights reserved.

DOI 10.1016/j.sbi.2004.06.003

Abbreviations

G2P glycerol-2-phosphate
G3P glycerol-3-phosphate
GlpT bacterial glycerol-3-phosphate transporter
LacY bacterial lactose permease
MFS major facilitator superfamily
OxIT bacterial oxalate transporter
P_i inorganic phosphate
UhpT bacterial glucose-6-phosphate transporter

Introduction

Secondary active membrane transporters use an electrochemical gradient to drive substrate translocation across

the membrane [1]. Since the studies more than half a century ago by Widdas and Mitchell, over 100 families of secondary active membrane transporters have been identified [2,3]. The largest family by far is the major facilitator superfamily (MFS) [4–7], with more than 3600 members identified to date [8]. Members of this superfamily are ubiquitous in all three kingdoms of life and have diverse substrate specificity, transporting ions, sugars, sugar-phosphates, drugs, neurotransmitters, nucleosides, amino acids, peptides and other hydrophilic solutes. Many MFS proteins have medical or pharmacological relevance, including the three human vesicular glutamate transporters (VGluT1–3) in the presynaptic terminal [9], the mammalian glucose transporter Glut4 from muscle and adipose tissues, and bacterial drug efflux pumps, which confer antibiotic resistance [10]. For almost all MFS proteins, hydrophobicity analysis of the protein sequence and reporter-fusion experiments suggest a topology of twelve transmembrane α helices (H1–H12), with the two six-helix halves of each protein being related by weak sequence homology [7,11]. The only conserved sequences across the entire MFS are two signature sequences, RXXRR, located in loops L2–3 and L8–9 [11].

A secondary active transporter uses one of three possible driving forces for substrate translocation [1]. Uniporters transport one type of solute and are driven directly by the substrate gradient. The second type, symporters, pumps two or more types of solutes in the same direction simultaneously, using the electrochemical gradient of one of the solutes as the driving force. Antiporters are driven in a similar way to symporters, except the solutes are transported in opposite directions across the membrane. Over the years, the molecular mechanisms of secondary active membrane transporters have been investigated extensively by mutagenesis, biochemical and kinetic techniques. Several mechanistic models have been proposed that differ in the number of substrate-binding sites, as well as in the conformational changes required for substrate translocation. In 1952, Widdas proposed a mobile carrier model in which a protein binds to a hydrophilic substrate and moves to the other side of the membrane, where it would release the substrate [12]. This was the first deviation from the channel hypothesis, until then the only known model of membrane transport. In 1957, Patlak proposed the concept of alternating gates [13]. This concept was developed into the single binding site, alternating access mechanism in 1966 by Vidavav

[14]. In this mechanism, the transporter is believed to have two major alternating conformations, inward facing (C_i) and outward facing (C_o). Interconversion of the two conformations facilitates substrate translocation across the membrane. Many variations of this mechanism were suggested in the following years (for reviews, see [15]), mostly based on thermodynamic considerations and kinetic studies [16,17]. Still, some fundamental questions remained regarding the characteristics of the substrate-binding site, the coupling of the ion gradient with substrate transport and the conformational changes required for substrate translocation. Moreover, the extraordinary substrate diversity of MFS proteins needed explanation. To address these questions, high-resolution structural information from crystallography was required. However, besides the well-documented problems associated with membrane protein crystallization, MFS proteins suffer from additional difficulties due to their lack of a sizable extramembrane domain and their inherent structural flexibility, which is required for large-scale conformational changes during the transport cycle.

Here we review the recently determined 3.3 Å resolution crystal structure of GlpT [18,19,20**], the glycerol-3-phosphate (G3P) transporter from the *E. coli* inner membrane and an antiporter MFS protein (Figure 1). In combination with biochemical studies, the transporter structure suggests a mechanism of substrate translocation. Furthermore, this structure, along with the 3.5 Å structure of *E. coli* lactose permease (LacY) [21**], a lactose/ H^+ symporter, and the 6.5 Å structure of the oxalate/formate antiporter (OxIT) from *Oxalobacter formigenes* in a substrate-bound form [22**,23], answered some key questions about the mechanism of secondary active membrane transporters in general.

Biochemical studies of GlpT and its homologue UhpT

Uptake of G3P by *E. coli* was first studied by Lin in the 1960s [24]. In the cell, G3P serves both as a carbon and energy source, and as a precursor for phospholipid biosynthesis [25]. GlpT translocates G3P across the inner membrane into the cytoplasm in exchange for inorganic phosphate (P_i) [26,27]. Transport is driven by the P_i gradient; the cellular P_i concentration, being 4 mM for non-growing cells [28], is much higher than in the extracellular milieu. The turnover rate is 24 mol of P_i per mole of GlpT per second at 37°C [18]. In addition to G3P, the protein also transports glycerol-2-phosphate (G2P) and fosfomycin, the only known phosphate-based antibiotic. The substrates bind to the protein via their phosphate moiety; glycerol does not facilitate transport [18]. *E. coli* GlpT consists of 452 amino acids [29], the majority of which are embedded in the membrane (Figure 1d). It purifies as a monomer and also binds to substrates in detergent solution as a monomer [18]. A human G3P transporter (G3PP) was recently identified [30] that

shares 22% sequence identity and 36% similarity with the *E. coli* GlpT protein.

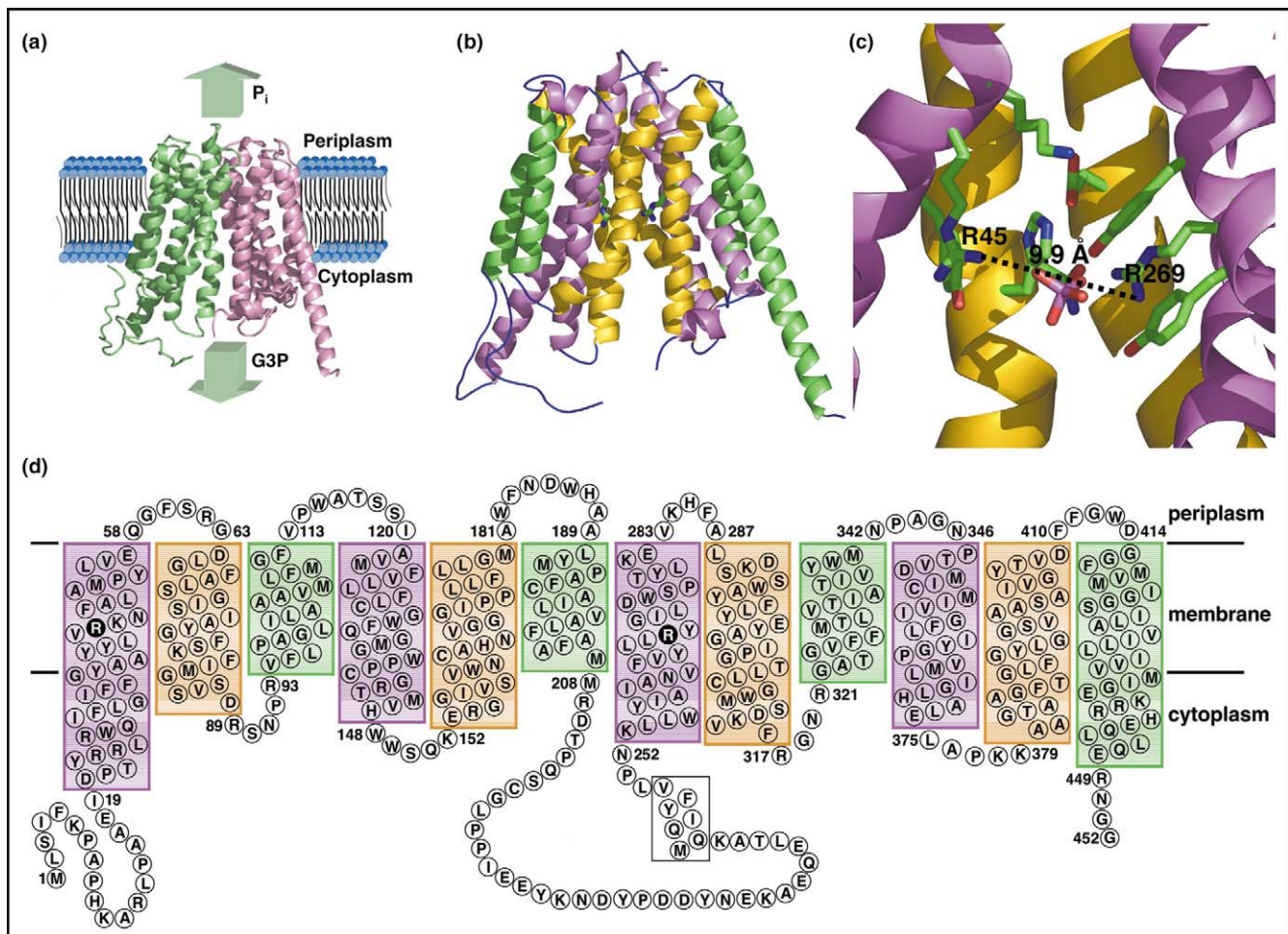
GlpT is closely related, both in function and in amino acid sequence, to another organic phosphate/inorganic phosphate antiporter, UhpT from *E. coli* [29,31], which carries out the electroneutral exchange of glucose-6-phosphate for P_i [32]. Extensive mutagenesis, biochemical and functional characterization has been carried out for UhpT, mostly by the Maloney group. Among all 14 arginine residues in the protein sequence, it was found that each of them could be replaced with a cysteine or a lysine without loss of function, except for Arg46 and Arg275 [33]. These two arginines were therefore proposed to lie at the substrate-binding site [33]. On the cytoplasmic side of residue Arg275, accessibility studies of single cysteine mutants showed that Cys265, Asn268, Ile269, Leu271 and Val273 of H7 line the substrate translocation pathway [34,35], and four of these five residues are conserved between UhpT and GlpT. On the other side of Arg275, residues Ile276, Thr283 and Val284 were found to be increasingly accessible to the periplasm in the outward-facing conformation [36]. Interestingly, based on the weak sequence homology between the N- and C-terminal halves, Maloney suggested in 1994 that an MFS protein would form two domains, with the substrate-binding site being located at the domain interface [6].

The affinity of GlpT and UhpT for organic phosphates is higher than that for P_i . In detergent solution, the K_d of GlpT for G3P, G2P and P_i are 3.64, 0.34 and 9.18 mM, respectively, as measured by tryptophan fluorescence quenching [18]. For UhpT in both right-side-out and inside-out vesicles, representing the C_o and C_i conformations of the protein, respectively, its affinity for organic phosphates is 10–20 times higher than that for P_i [37]. In addition, the affinity for a given substrate changes by only a factor of two between the two conformations, indicating overall functional symmetry.

GlpT structure

The GlpT molecule, with the shape of a Mayan temple, is composed of N- and C-terminal domains, each consisting of a compact six-helix bundle [20**]. The N- and C-terminal halves are related by a central pseudo-twofold symmetry axis perpendicular to the membrane plane (Figures 1a and 2a). The $C\alpha$ rmsd between the two domains is 2.43 Å, reflecting the weak homology between the two halves of the protein sequence [29]. The central loop linking the two domains is long, whereas most loops connecting the transmembrane α helices of both domains are very short, leaving little freedom for relative movement of the helices within each domain. The high glycine content in the transmembrane region ensures close packing of the α helices within their domains [38]. The interactions between the N- and C-terminal domains, however, are relatively weak. Although there is extensive

Figure 1



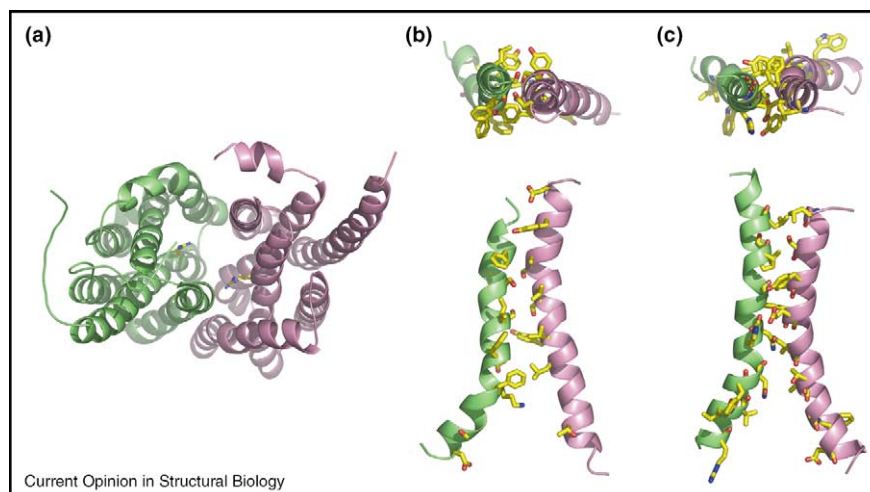
Structure of GlpT (adapted from [20**]). **(a)** Ribbon representation of GlpT viewed from within the membrane. The GlpT molecule measures ~ 35 Å by 45 Å at the top and 35 Å by 60 Å at the bottom, and its height is ~ 60 Å. The N-terminal domain is colored green and the C-terminal domain is pink. **(b)** The 12 transmembrane α helices are designated H1 to H12, and their connecting loops L1–2 to L11–12. Four peripheral helices (H3, H6, H9 and H12) that are not involved in pore formation are colored green, whereas the four that line the central pore (H2, H5, H8, and H11) are colored yellow. The four central helices (H1, H4, H7 and H10) are colored purple. Arg45 from H1 and Arg269 from H7, key residues for substrate binding, are located at the closed end of the substrate translocation pathway in the middle of the membrane. **(c)** Substrate-binding site. The shortest distance between the guanidinium groups of Arg45 and Arg269 is 9.9 Å. **(d)** Wild-type amino acid sequence and transmembrane topology of GlpT. The N- and C-terminal halves of the protein have weak sequence homology. Residues Arg45 in H1 and Arg269 in H7 are indicated in bold in the sequence. The program PyMol [61] was used to prepare (a–c) and most other figures in this review.

van der Waals contact between the domains at their interface, no salt bridges and few hydrogen bonds exist. The Lys46 sidechain, although positioned at the domain interface not far from Asp274 of the C-terminal domain (Figure 2a), actually had no electron density associated with it and was therefore disordered in the structure.

The substrate translocation pathway in GlpT is visualized as a pore located between the N- and C-terminal domains [20**]. The pore is surrounded by eight transmembrane α helices: H1 and H4, and H7 and H10 on the two sides; H2 and H11 in the front; and H5 and H8 in the back (Figure 1b,d). The pore is open to the cytoplasm and closed to the periplasm, and therefore the GlpT

structure represents its inward-facing conformation, C_i . Because substrate binding is via the negatively charged phosphate moiety, the substrate-binding site is expected to have positive electrostatic surface potential. Arg45 from H1 and Arg269 from H7 are found at the closed end of the otherwise hydrophobic pore in the middle of the membrane (Figure 1c). These two positively charged residues are proposed to form the substrate-binding site. Interestingly, these two residues are the equivalent of the two essential arginines in UhpT [33]. Such coordination of phosphate by two arginine sidechains is similar to that seen in the fosfomycin-binding site of the MurA protein [39]. Our preliminary docking experiments showed that G3P binding is indeed coordinated by

Figure 2



Interface of the N- and C-terminal domains. **(a)** GlpT structure viewed from the cytoplasm. **(b,c)** Helices at the N- and C-terminal domain interface, viewed from the periplasm and from within the membrane plane. As the four helices are curved into a banana-like shape, each pair has the shape of an hourglass, with the helices making contact within the membrane but being separated from each other in the cytoplasm.

Arg45 and Arg269. The sidechains of both arginines are rigidly held in space, as each is surrounded by five residues: Arg45 by Try38, Lys46, Try42, Gln134, His165 and Try393; and Arg269 by His165, Asn166, Try266, Try270, Glu299 and Try362.

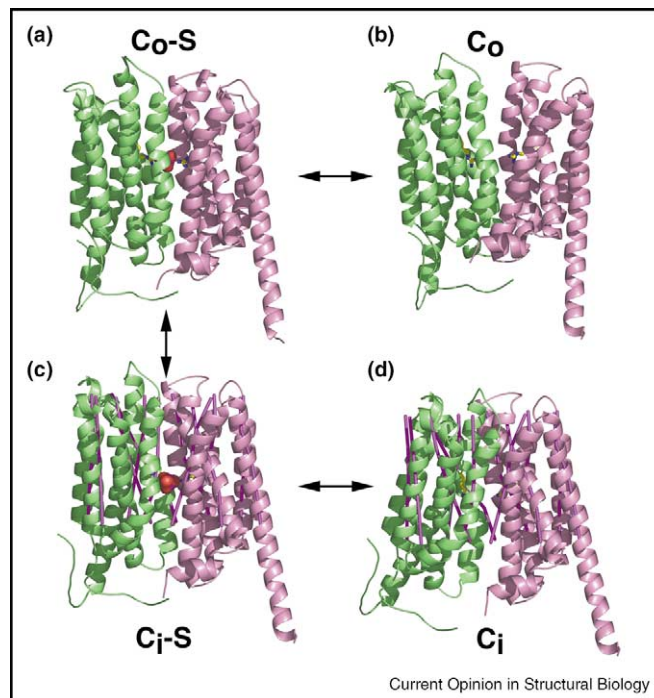
Conformational change associated with substrate translocation

Two pairs of transmembrane α helices at the domain interface are highly curved [20^{••}], and the MSF signature sequences are probably involved in maintaining their curvature. Both the front pair of helices, H2 and H11, and the back pair, H5 and H8, are curved such that the N- and C-terminal domains both have a convex surface at their interface (Figure 2b,c). These helices are also highly distorted, partially due to their high glycine content. Interestingly, helix curvature is not caused by proline residues. Instead, the short loops at the ends of these helices, together with support from those helices in each domain that the interface helices intersect with, are probably responsible for maintaining their curvature (Figure 2). For comparison, the corresponding helices in the LacY [21^{••}] and OxIT [22^{••}] structures are similarly curved. Two of the loops connected to the interface helices, L2–3 and L8–9, consist of the RXXRR signature sequence of the MFS [11], whose significance has been unclear. In addition to their role in preserving the transmembrane topology of MFS proteins [40], we propose that, as short loops with positively charged residues at both ends, they are involved in maintaining the curvature of the interface helices. The curvature of these helices (Figure 2b,c), packed back-to-back at the interface, is probably important for the conformational changes associated with substrate translocation.

Our biochemical experiments showed that GlpT undergoes conformational changes upon substrate binding [20^{••}]. Residues Asn232–Leu239 in the long central loop connecting the N- and C-terminal halves were disordered in the crystal structure. In both inside-out membrane vesicles and detergent solution, this loop was sensitive to trypsin cleavage at Lys234 [20^{••}]. Interestingly, trypsin cleavage of the loop was inhibited by the presence of G3P, or P_i at higher concentrations, indicating a substrate-binding-induced conformational change in the loop connecting the N- and C-terminal domains. The binding of either G3P or P_i also caused quenching of tryptophan fluorescence signals [18]. Furthermore, the Stokes radius of GlpT in detergent solution was reduced upon the addition of G3P [20^{••}]. Taken together, these experiments suggest that GlpT changes to a more compact conformation when substrate is bound.

Comparison of the GlpT structure with the 6.5 Å map of OxIT in a substrate-bound form [22^{••}] suggests possible conformational changes associated with substrate translocation (Figure 3). Because the interactions of the N- and C-terminal domains in GlpT are weak, the curvature of the helices at the domain interface (Figure 2b,c) would allow a rocker-switch type of movement between the two domains. The periplasmic ends of these helices would separate as their cytoplasmic ends move closer together. In fact, by separately rotating the two halves of the GlpT model in opposite directions along an axis at their interface and parallel to the membrane (Figure 3c,d), we found that an $\sim 6^\circ$ rotation of each domain can generate a structure similar to the substrate-bound form of OxIT [22^{••}]. An additional $\sim 4^\circ$ rotation of each domain is sufficient to close the pore on the cytosolic side of the molecule and,

Figure 3



Proposed rocker-switch type conformational changes accompany substrate translocation by GlpT. The crystal structure **(d)** represents the C_i conformation of the protein. The C_i - P_i conformation **(c)** was generated by fitting the GlpT model into the 6.5 Å map of the substrate-bound form of OxIT [22**], the latter being represented by elongated rods. By separately rotating the two halves of the GlpT model in opposite directions along an axis at their interface and parallel to the membrane, we found that an $\sim 6^\circ$ rotation of each domain can generate a structure that fits the OxIT map reasonably well. The C_o - P_i conformation **(a)** was produced by an $\sim 10^\circ$ rotation of each domain that is sufficient to close the pore on the cytosolic side of the molecule and to open a pore on the periplasmic side. Finally, the C_o conformation **(b)** was generated by a 16° rotation.

at the same time, to expose the substrate-binding site to the periplasm (Figure 3a). This is in contrast to the total 60° rotation proposed for LacY during transport [21**], for which the substrate lactose is significantly larger. For transporters of much smaller substrates, such as the Cl^-/H^+ antiporter CIC-ec1 from *E. coli*, the conformational changes required for substrate translocation are also expected to be much smaller, probably involving only the movement of sidechains at the binding site [41,42].

Mechanism of substrate translocation

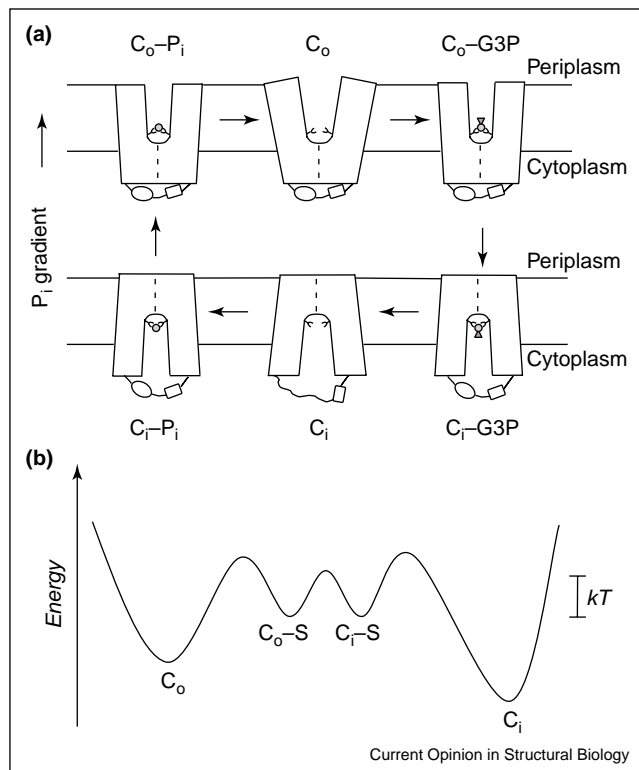
The GlpT crystal structure and biochemical data on GlpT and UhpT suggest that the transporter operates via a single binding site, alternating access mechanism with a rocker-switch type of movement of the N- and C-terminal domains (Figure 4a) [20**]. In the inward-facing conformation of GlpT, the shortest distance between Arg45 and Arg269 at the substrate-binding site is about 9.9 Å (Figure 1c). This is 1.4 Å longer than required for a bound phosphate to form optimal hydrogen bonds simultaneously with both arginines. We proposed that P_i binding pulls these two arginines apart, thus moving the N- and C-terminal domains closer and narrowing the cytoplasmic pore (Figure 2a). Substrate binding also

destabilizes the interface between the N- and C-terminal domains on the periplasmic side and allows further tilting of the two domains to expose the substrate-binding site to the periplasm, yielding the C_o conformation. In the periplasm, the lower affinity of the transporter for P_i [18,24] allows its replacement by G3P, whereas in the cytoplasm P_i replaces G3P at the binding site due to its much higher cytosolic concentration. In other words, substrate binding lowers the energy barrier between the C_i and C_o conformations of GlpT, and the two substrate-bound complexes for each substrate (S), C_i -S and C_o -S, have similar energy levels (Figure 4b). This allows their interconversion by Brownian motion and thus the P_i gradient can drive G3P transport by GlpT. Unlike what is postulated in the case of some primary active membrane transporters [17], no large difference in the affinity of a transporter for a substrate on the different sides of the membrane is required for translocation.

GlpT as a structural and mechanistic model for other MFS proteins

The structures of GlpT [20**] and LacY [21**] are quite similar, with an rmsd of 2.84 Å between the positions of 64% of their $C\alpha$ atoms. The 6.5 Å OxIT map, determined

Figure 4



Proposed single binding site, alternating access mechanism with a rocker-switch type of movement. (a) Reaction cycle of substrate translocation [20**]. The positions of Arg45 and Arg269 are indicated. P_i is represented by a small disk, and the G3P molecule by a small disk and a triangle. (b) Schematic drawing to illustrate the free energy levels of various conformations of GlpT in the translocation cycle. S denotes substrate.

by cryo-electron microscopy from reconstituted two-dimensional crystals, also suggests a similar architecture [22**,23]. Thus, all three MFS protein structures solved to date have the same topology and structural design. Such structural similarity is particularly noteworthy given the absence of significant sequence homology, with only 12–14% sequence identity between any two of the three proteins. On the other hand, proteins from other secondary active membrane transporter families — the erythrocyte anion exchanger [43], the Na^+/H^+ antiporter NhaA [44], the multidrug transporter AcrB [45], the melibiose permease MelB [46], the Na^+ /betaine symporter BetP [47], the mitochondrial ADT/ATP carrier [48] and the bacterial small multidrug efflux protein EmrE [49,50] — all appear to have different three-dimensional structures. This clearly validates the membrane transport protein classification scheme by Saier, Paulsen and colleagues [2,3]. It follows that proteins in each family or superfamily have the same ancestor in evolution and, therefore, share the same architecture and similar molecular mechanisms.

The structures of GlpT [20**] and LacY [21**] are likely to be a paradigm for other MFS proteins. The substrate translocation pathway is located at the N- and C-terminal domain interface, formed by eight transmembrane α helices, with the substrate-binding site located at the domain interface. Such a structural model agrees with the large amounts of biochemical data available for various MFS proteins, including the erythrocyte glucose transporter Glut1 [51], the tetracycline transporter TetA [52], the yeast high-affinity glucose transporter Hxt2 [53] and the rat vesicular monoamine transporter rVMAT2 [54]. In the transporter structure, only a few key residues are involved in substrate binding and their substitution can change the substrate specificity of the transporter, as has been observed for LacY [55] and UhpT [56]. This explains the extraordinary substrate diversity of members of the MFS.

Unlike GlpT and LacY [20**,21**], both of which work as a monomer, some MFS proteins, such as the lactose transporter LacS from *Streptococcus thermophilus* [57] and the tetracycline transporter TetL from *Bacillus subtilis* [58], form a dimer in the membrane and in detergent solution. As all MFS proteins share a similar topology and even some degree of sequence homology, it is likely that they all have the ability to work as monomers and have their substrate translocation pore located between the N- and C-terminal halves of the protein. In an oligomer, the large-scale conformational changes between the two halves of the MFS protein required for substrate translocation mean that transport by one monomer is likely to affect the activity of the other(s). It follows that various monomers would be expected to function cooperatively. In the case of TetL, the two monomers in a dimer associate very tightly [58]. Given the gross conformational changes expected, this suggests that the two monomers work in an ‘in-phase’, as opposed to ‘out-of-phase’, manner. Such oligomerization provides another dimension of regulation (e.g. by allosteric interactions).

The three modes of secondary active membrane transport — uniport, symport and antiport — are clearly related in their kinetic schemes [1]. Furthermore, Maloney has suggested the possibility of a united mechanism for the three types of transport modes [6,59]. A single binding site, alternating access mechanism with a rocker-switch type of movement of the N- and C-terminal domains has been proposed for GlpT, an antiporter (Figures 3 and 4) [20**]. Such a mechanism, with minor modifications, can also account for substrate translocation by uniporters and symporters of the MFS. We propose that all three types of transporters share the characteristic that substrate binding lowers the energy barrier between the inward- and outward-facing conformations, and speeds up their interconversion. Thus, a substrate or ion gradient can drive transport. For a uniporter, the energy barrier between the C_i and C_o conformations is small enough that their

interconversion can occur without a substrate bound. Nonetheless, substrate binding would further reduce this small energy barrier and accelerate their interconversion. Such a mechanism would predict the existence of an exchange process that is faster than net transport, as has actually been observed for Glut1 [60]. For a symporter, it is the simultaneous binding of two substrates that is required to lower the energy barrier between the C_i and C_o conformations. Perhaps the simplicity of both the structural and mechanistic design of an MFS protein, as shown for GlpT, makes it a popular choice by Nature for transporting various substrates across the membrane of the cell.

Conclusions

Together with mutagenesis and biochemical data, the 3.3 Å crystal structure of GlpT from *E. coli* [18,19,20**] suggests a substrate translocation mechanism for the transporter. Both the three-dimensional structure and its substrate translocation mechanism are likely to be a paradigm for other members of the MFS. In addition to solving the transporter structure in its outward-facing and substrate-bound conformations, future directions include testing the proposed substrate translocation mechanism [20**] using mutagenesis, functional assays and spectroscopic approaches. An even more challenging task is to determine the structures of the human membrane transporters that are directly involved in the pathogenesis of diseases in order to understand their mechanisms.

Acknowledgements

We thank other previous or current members of our laboratory for contributing to the project: M Auer, MJ Kim, XD Li, JM Song, A Villa and X Zhang. We are grateful to PC Maloney and TA Krulwich for inspiring discussion on membrane transport mechanisms. D-NW thanks R Reithmeier for introducing him to the membrane transport field. This work was financially supported by the National Institutes of Health (RO1-DK53973 and RO1-GM052837) and by the Diabetes Research Bridging Fund of the New York State Department of Health.

References and recommended reading

Papers of particular interest, published within the annual period of review, have been highlighted as:

- of special interest
- of outstanding interest

1. Mitchell P: **Molecule, group and electron translocation through the natural membranes.** *Biochem Soc Symp* 1963, **22**:141-168.
 2. Paulsen IT, Sliwinski MK, Saier Jr MH: **Microbial genome analyses: global comparisons of transport capabilities based on phylogenies, bioenergetics and substrate specificities.** *J Mol Biol* 1998, **277**:573-592.
 3. Paulsen IT, Nguyen L, Sliwinski MK, Rabus R, Saier Jr MH: **Microbial genome analyses: comparative transport capabilities in eighteen prokaryotes.** *J Mol Biol* 2000, **301**:75-100.
 4. Reizer J, Finley K, Kakuda D, MacLeod CL, Reizer A, Saier Jr MH: **Mammalian integral membrane receptors are homologous to facilitators and antiporters of yeast, fungi, and eubacteria.** *Protein Sci* 1993, **2**:20-30.
 5. Henderson PJF: **The 12-transmembrane helix transporters.** *Curr Opin Cell Biol* 1993, **5**:708-712.
 6. Maloney PC: **Bacterial transporters.** *Curr Opin Cell Biol* 1994, **6**:571-582.
 7. Pao SS, Paulsen IT, Saier Jr MH: **Major facilitator superfamily.** *Microbiol Mol Biol Rev* 1998, **62**:1-34.
 8. Ren Q, Kang KH, Paulsen IT: **TransportDB: a relational database of cellular membrane transport systems.** *Nucleic Acids Res* 2004, **32**:D284-D288.
 9. Takamori S, Rhee JS, Rosenmund C, Jahn R: **Identification of a vesicular glutamate transporter that defines a glutamatergic phenotype in neurons.** *Nature* 2000, **407**:189-194.
 10. Levy SB: **Active efflux, a common mechanism for biocide and antibiotic resistance.** *J Appl Microbiol* 2002, **92**:65S-71S.
 11. Maiden MC, Davis EO, Baldwin SA, Moore DC, Henderson PJ: **Mammalian and bacterial sugar transport proteins are homologous.** *Nature* 1987, **325**:641-643.
 12. Widdas WF: **Inability of diffusion to account for placental glucose transfer in the sheep and consideration of the kinetics of a possible carrier transfer.** *J Physiol* 1952, **118**:23-39.
 13. Patlak C: **Contributions to the theory of active transport: II. The gate type non-carrier mechanism and generalizations concerning tracer flow, efficiency, and measurement of energy expenditure.** *Bull Math Biophys* 1957, **19**:209-235.
 14. Vidavav GA: **Inhibition of parallel flux and augmentation of counter flux shown by transport models not involving a mobile carrier.** *J Theor Biol* 1966, **10**:301-306.
 15. West IC: **Ligand conduction and the gated-pore mechanism of transmembrane transport.** *Biochim Biophys Acta* 1997, **1331**:213-234.
 16. Jencks WP: **The utilization of binding energy in coupled vectorial processes.** *Adv Enzymol Relat Areas Mol Biol* 1980, **51**:75-106.
 17. Tanford C: **Mechanism of free energy coupling in active transport.** *Annu Rev Biochem* 1983, **52**:379-409.
 18. Auer M, Kim MJ, Lemieux MJ, Villa A, Song J, Li XD, Wang DN: **High-yield expression and functional analysis of *Escherichia coli* glycerol-3-phosphate transporter.** *Biochemistry* 2001, **40**:6628-6635.
 19. Lemieux MJ, Song J, Kim MJ, Huang Y, Villa A, Auer M, Li XD, Wang DN: **Three-dimensional crystallization of the *Escherichia coli* glycerol-3-phosphate transporter: a member of the major facilitator superfamily.** *Protein Sci* 2003, **12**:2748-2756.
 20. Huang Y, Lemieux MJ, Song J, Auer M, Wang DN: **Structure and mechanism of the glycerol-3-phosphate transporter from *Escherichia coli*.** *Science* 2003, **301**:616-620.
- The 3.3 Å resolution structure of GlpT from *E. coli* reveals 12 transmembrane α helices forming N- and C-terminal domains with pseudo-twofold symmetry. Between the two domains, two arginine sidechains constitute the substrate-binding site. The transporter is in its inward-facing, unliganded conformation. In combination with biochemical experiments, the structure suggests a single binding site, alternating access mechanism with a rocker-switch type of movement.
21. Abramson J, Smirnova I, Kasho V, Verner G, Kaback HR, Iwata S: **Structure and mechanism of the lactose permease of *Escherichia coli*.** *Science* 2003, **301**:610-615.
- This paper describes the 3.5 Å crystal structure of LacY from *E. coli*. The twelve transmembrane α helices of the protein form two six-helix bundles. A substrate analog bound between the bundles reveals the substrate-binding site and the residues involved. The transporter is in its inward-facing conformation. The structure provides a framework to understand the vast amounts of biochemical data available on the protein.
22. Hirai T, Heymann JA, Shi D, Sarker R, Maloney PC, Subramaniam **S: Three-dimensional structure of a bacterial oxalate transporter.** *Nat Struct Biol* 2002, **9**:597-600.
- The 6.5 Å resolution structure of OxIT determined by cryo-electron microscopy of two-dimensional crystals grown in the presence of substrate revealed 12 transmembrane α helices surrounding a central pore. This was the first time that the transmembrane α helices of an MFS protein were visualized, proving the 12-helix topology predicted from the protein sequence.

23. Hirai T, Heymann JA, Maloney PC, Subramaniam S: **Structural model for 12-helix transporters belonging to the major facilitator superfamily.** *J Bacteriol* 2003, **185**:1712-1718.
24. Hayashi S, Koch JP, Lin ECC: **Active transport of L- α -glycerophosphate in *Escherichia coli*.** *J Biol Chem* 1964, **239**:3098-3105.
25. Rock CO, Cronan JE: **Lipid metabolism in prokaryotes.** In *Biochemistry of Lipids and Membranes*. Edited by Vance DE, Vance JE. San Francisco: Benjamin/Cummings; 1985:73-115.
26. Elvin CM, Hardy CM, Rosenberg H: **P_i exchange mediated by the GlpT-dependent sn-glycerol-3-phosphate transport system in *Escherichia coli*.** *J Bacteriol* 1985, **161**:1054-1058.
27. Ambudkar SV, Larson TJ, Maloney PC: **Reconstitution of sugar phosphate transport systems of *Escherichia coli*.** *J Biol Chem* 1986, **261**:9083-9086.
28. Vink R, Bendall MR, Simpson SJ, Rogers PJ: **Estimation of H⁺ to adenosine 5'-triphosphate stoichiometry of *Escherichia coli* ATP synthase using 31P NMR.** *Biochemistry* 1984, **23**:3667-3675.
29. Eiglmeier K, Boos W, Cole ST: **Nucleotide sequence and transcriptional startpoint of the glpT gene of *Escherichia coli*: extensive sequence homology of the glycerol-3- phosphate transport protein with components of the hexose-6-phosphate transport system.** *Mol Microbiol* 1987, **1**:251-258.
30. Bartoloni L, Wattenhofer M, Kudoh J, Berry A, Shibuya K, Kawasaki K, Wang J, Asakawa S, Talior I, Bonne-Tamir B *et al.*: **Cloning and characterization of a putative human glycerol 3-phosphate permease gene (SLC37A1 or G3PP) on 21q22.3: mutation analysis in two candidate phenotypes, DFNB10 and a glycerol kinase deficiency.** *Genomics* 2000, **70**:190-200.
31. Maloney PC, Ambudkar SV, Anatharam V, Sonna LA, Varadhachary A: **Anion-exchange mechanisms in bacteria.** *Microbiol Rev* 1990, **54**:1-17.
32. Sonna LA, Ambudkar SV, Maloney PC: **The mechanism of glucose 6-phosphate transport by *Escherichia coli*.** *J Biol Chem* 1988, **263**:6625-6630.
33. Fann MC, Davies AH, Varadhachary A, Kuroda T, Sevier C, Tsuchiya T, Maloney PC: **Identification of two essential arginine residues in UhpT, the sugar phosphate antiporter of *Escherichia coli*.** *J Membr Biol* 1998, **164**:187-195.
34. Yan RT, Maloney PC: **Identification of a residue in the translocation pathway of a membrane carrier.** *Cell* 1993, **75**:37-44.
35. Yan RT, Maloney PC: **Residues in the pathway through a membrane transporter.** *Proc Natl Acad Sci USA* 1995, **92**:5973-5976.
36. Matos M, Fann MC, Yan RT, Maloney PC: **Enzymatic and biochemical probes of residues external to the translocation pathway of UhpT, the sugar phosphate carrier of *Escherichia coli*.** *J Biol Chem* 1996, **271**:18571-18575.
37. Fann MC, Maloney PC: **Functional symmetry of UhpT, the sugar phosphate transporter of *Escherichia coli*.** *J Biol Chem* 1998, **273**:33735-33740.
38. Liu Y, Engelman DM, Gerstein M: **Genomic analysis of membrane protein families: abundance and conserved motifs.** *Genome Biol* 2002, **3**:54.
39. Skarzynski T, Mistry A, Wonacott A, Hutchinson SE, Kelly VA, Duncan K: **Structure of UDP-N-acetylglucosamine enolpyruvyl transferase, an enzyme essential for the synthesis of bacterial peptidoglycan, complexed with substrate UDP-N-acetylglucosamine and the drug fosfomicin.** *Structure* 1996, **4**:1465-1474.
40. Sato M, Mueckler M: **A conserved amino acid motif (R-X-G-R-R) in the Glut1 glucose transporter is an important determinant of membrane topology.** *J Biol Chem* 1999, **274**:24721-24725.
41. Dutzler R, Campbell EB, Cadene M, Chait BT, MacKinnon R: **X-ray structure of a ClC chloride channel at 3.0 Å reveals the molecular basis of anion selectivity.** *Nature* 2002, **415**:287-294.
42. Accardi A, Miller C: **Secondary active transport mediated by a prokaryotic homologue of ClC Cl⁻ channels.** *Nature* 2004, **427**:803-807.
43. Wang DN, Sarabia VE, Reithmeier AF, Kühlbrandt W: **Three-dimensional map of the dimeric membrane domain of the human erythrocyte anion exchanger, Band 3.** *EMBO J* 1994, **13**:3230-3235.
44. Williams KA: **Three-dimensional structure of the ion-coupled transport protein NhaA.** *Nature* 2000, **403**:112-115.
45. Murakami S, Nakashima R, Yamashita E, Yamaguchi A: **Crystal structure of bacterial multidrug efflux transporter AcrB.** *Nature* 2002, **419**:587-593.
46. Hacksell I, Rigaud JL, Purhonen P, Poyrcher T, Hebert H, Leblanc G: **Projection structure at 8 Å resolution of the melibiose permease, an Na-sugar co-transporter from *Escherichia coli*.** *EMBO J* 2002, **21**:3569-3574.
47. Ziegler C, Morbach S, Schiller D, Kramer R, Tziatzios C, Schubert D, Kühlbrandt W: **Projection structure and oligomeric state of the osmoregulated sodium/glycine betaine symporter BetP of *Corynebacterium glutamicum*.** *J Mol Biol* 2004, **337**:1137-1147.
48. Pebay-Peyroula E, Dahout-Gonzalez C, Kahn R, Trezeguet V, Lauquin GJ, Brandolin G: **Structure of mitochondrial ADP/ATP carrier in complex with carboxyatractyloside.** *Nature* 2003, **426**:39-44.
49. Ubarretxena-Belandia I, Baldwin JM, Schuldiner S, Tate CG: **Three-dimensional structure of the bacterial multidrug transporter EmrE shows it is an asymmetric homodimer.** *EMBO J* 2003, **22**:6175-6181.
50. Ma C, Chang G: **Structure of the multidrug resistance efflux transporter EmrE from *Escherichia coli*.** *Proc Natl Acad Sci USA* 2004, **101**:2852-2857.
51. Mueckler M, Makepeace C: **Analysis of transmembrane segment 8 of the GLUT1 glucose transporter by cysteine-scanning mutagenesis and substituted cysteine accessibility.** *J Biol Chem* 2004, **279**:10494-10499.
52. Tamura N, Konishi S, Iwaki S, Kimura-Someya T, Nada S, Yamaguchi A: **Complete cysteine-scanning mutagenesis and site-directed chemical modification of the Tn10-encoded metal-tetracycline/H⁺ antiporter.** *J Biol Chem* 2001, **276**:20330-20339.
53. Kasahara T, Kasahara M: **Transmembrane segments 1, 5, 7 and 8 are required for high-affinity glucose transport by *Saccharomyces cerevisiae* Hxt2 transporter.** *Biochem J* 2003, **372**:247-252.
54. Verdy E, Arkin IT, Gottschalk KE, Kaback HR, Schuldiner S: **Structural conservation in the major facilitator superfamily as revealed by comparative modeling.** *Protein Sci* 2004, in press.
55. Olsen SG, Greene KM, Brooker RJ: **Lactose permease mutants which transport (malto)-oligosaccharides.** *J Bacteriol* 1993, **175**:6269-6275.
56. Hall JA, Fann MC, Maloney PC: **Altered substrate selectivity in a mutant of an intrahelical salt bridge in UhpT, the sugar phosphate carrier of *Escherichia coli*.** *J Biol Chem* 1999, **274**:6148-6153.
57. Veenhoff LM, Heuberger EH, Poolman B: **The lactose transport protein is a cooperative dimer with two sugar translocation pathways.** *EMBO J* 2001, **20**:3056-3062.
58. Safferling M, Griffith H, Jin J, Sharp J, De Jesus M, Ng C, Krulwich TA, Wang DN: **The TetL tetracycline efflux protein from *Bacillus subtilis* is a dimer in the membrane and in detergent solution.** *Biochemistry* 2003, **42**:13969-13976.
59. Maloney PC, Wilson TH: **Ion-coupled transport and transporters.** In *Escherichia coli and Salmonella: Cellular and Molecular Biology*, edn 2. Edited by Neidhardt FC, Curtiss RI, Ingraham JL, Lin ECC, Low KB, Magasanik B, Reznikoff WS, Riley M, Schaechter M, Umberger HE. Washington, DC: ASM Press; 1996:1130-1148.
60. Kasahara M, Hinkle PC: **Reconstitution of D-glucose transport catalyzed by a protein fraction from human erythrocytes in sonicated liposomes.** *Proc Natl Acad Sci USA* 1976, **73**:396-400.
61. DeLano WL: *The PyMOL User's Manual*. San Carlos, CA: DeLano Scientific; 2002.